JGR Atmospheres

RESEARCH ARTICLE
10.1029/2018JD030230

Amplified Urban Heat Islands during Heat Wave Periods

Shaojing Jiang[1,2], Xuhui Lee[3], Jiankai Wang[2], and Kaicun Wang[1]

[1]State Key Laboratory of Earth Surface Processes and Resource Ecology, College of Global Change and Earth System Science, Beijing Normal University, Beijing, China, [2]Chinese Academy of Meteorological Sciences, Beijing, China, [3]School of Forestry and Environmental Studies, Yale University, New Haven, CT, USA

Key Points:
- Heat waves intensified nighttime UHIs by 0.9 ± 0.36 and 0.8 ± 0.20 °C in Beijing and Guangzhou, respectively, and by 0.9±0.13 °C for daytime UHIs in Shanghai
- Increased surface solar radiation during the heat wave period may be the primary cause of the intensified nighttime UHIs in Beijing and Guangzhou
- Changes in wind direction may have a strong contribution to the intensified daytime UHIs in Shanghai during heat wave periods

Supporting Information:
- Supporting Information S1

Correspondence to:
K. Wang,
kcwang@bnu.edu.cn

Citation:
Jiang, S., Lee, X., Wang, J., & Wang, K. (2019). Amplified urban heat islands during heat wave periods. *Journal of Geophysical Research: Atmospheres*, *124*, 7797–7812. https://doi.org/10.1029/2018JD030230

Received 28 DEC 2018
Accepted 30 JUN 2019
Accepted article online 12 JUL 2019
Published online 29 JUL 2019

Abstract Heat waves and urban heat islands (UHIs) may interact together, but the dependence of their interaction on background climate is unclear. Hourly meteorological observations in June to August from 2013 to 2015 collected in the megacities of Beijing (temperate semihumid monsoon climate), Shanghai (subtropical humid monsoon climate), and Guangzhou (marine subtropical monsoon climate) in China were used to study the interaction. At each megacity, eight rural stations and eight urban stations, respectively, were selected to study the UHI. Although under different background climates, UHIs in Beijing and Guangzhou shared a similar diurnal variability, that is, higher in the nighttime. However, the diurnal cycle is opposite for Shanghai if rural coastal stations were selected as rural reference stations. During heat wave periods, daytime (10:00–16:00) UHIs were intensified by 0.9 ± 0.13 (mean ± 1 standard deviation) °C in Shanghai, nighttime (22:00–4:00) UHIs were intensified by 0.9 ± 0.36 and 0.8 ± 0.20 °C in Beijing and Guangzhou, respectively. The surface solar radiation during the heat wave period was approximately 1.5 times to that under normal conditions in each city. The enhanced solar radiation during heat waves, which was absorbed by the urban canopy in the daytime and released at night, was closely related to nighttime UHIs in Beijing and Guangzhou and daytime UHIs in Shanghai. Additionally, changes in wind direction were observed in Shanghai under heat waves, that is, with more than 63% (wind direction) of the wind originating from neighboring hot cities in the southwest instead of the cool sea breeze from the southeast, which led to a significant increase in daytime UHIs during heat wave periods.

Plain Language Summary Heat waves are one of the most damaging natural disasters in the world. Generally, urban areas tend to experience more severe heat stress under heat waves due to the urban heat island (UHI) effect (i.e., urban areas being warmer than rural areas). The impacts of heat waves on UHIs under different local background climates remain unclear, especially for the diurnal cycles of UHIs. In this study, hourly UHIs were analyzed under heat waves in three megacities: Beijing, Shanghai, and Guangzhou. The results show that nighttime UHIs were obviously intensified in Beijing and Guangzhou under heat waves, whereas in Shanghai, the intensified UHIs were much stronger during daytime than during nighttime. Increased solar radiation under heat waves was an important factor for the amplified UHIs. In addition, changes in wind direction also played an essential role in the intensified daytime UHIs in Shanghai.

1. Introduction

The urban heat island (UHI) is a phenomenon that urban areas have higher temperatures than have the surrounding rural areas (Voogt & Oke, 2003). It has been pointed out that the primary factors that control UHIs are land cover change, urban expansion, and anthropogenic heat (Stewart & Oke, 2012), which reduce the evaporative cooling efficiency and increase the storage and release of heat in urban areas (Arnfield, 2003; Zhou et al., 2016). Urban expansion has been predicted to increase throughout the world in the future, especially in developing countries, whose urban land cover is expected to reach 1.2 $\times 10^6$ km^2 in 2050 (Angel et al., 2011). Moreover, cities tend to experience increased heat stress due to their large footprints and strong UHI effects, which result from increasing urban expansion (Luo & Lau, 2018; Wang, Huang, et al., 2016; Zhao, 2018; Zhou et al., 2015).

A heat wave is a period of consecutive hot days (Kuglitsch et al., 2010) and is recognized as one of the deadliest natural disasters (Poumadère et al., 2005; Semenza et al., 1996). More frequent and severe heat waves are expected to occur in the future due to the background of continued global warming (Lewis et al., 2017; Meehl & Tebaldi, 2004) and urbanization (Yang, Ruby Leung, et al., 2017). Approximately

Table 1
The Local Background Climate, Urbanization Statistics, and Heat Wave Conditions in Beijing, Shanghai, and Guangzhou From 2013 to 2015

	City		
Geographic information	Beijing	Shanghai	Guangzhou
Downtown location	116.4°E, 39.9°N	121.1°E, 31.1°N	113.3°E, 23.1°N
Climatic zone	Temperate semihumid monsoon	Subtropical humid monsoon	Marine subtropical monsoon
Total areas (km^2)	16,410	6,340	7,434
Main urban area (km^2)	1401	1364	785
Population in 2015 (million)	21.71	24.15	13.50
Urban mean elevation (m)	43.5	5.5	37.5
Heat waves (days)	30	50	91
Normal conditions (days)	129	137	55
Urban temperature stations	8	8	8
Rural temperature stations	8	8	8

54% of the world's population already live in cities, and this number is predicted to reach 70% by 2050 (United Nations, 2014). Therefore, increasing risks of heat-related deaths and illnesses as well as increasing demands for power (Huang et al., 2010; Ke et al., 2016; Kovats & Kristie, 2006) exist in urban areas (Wouters et al., 2017).

The synergistic interaction between UHIs and heat waves has been studied in several regions, and most of these studies were based on observations or numerical simulations. Founda and Santamouris (2017) studied the heat waves during summer 2012 in Athens and reported a positive interaction between UHIs and heat waves; the UHI magnitude was intensified by up to 3.5 °C during heat waves. Li and Bou-Zeid (2013) analyzed the heat waves in Baltimore, Maryland, and Washington DC and concluded that the heat stress in urban areas was stronger than the sum of UHI effect and the heat wave effect. Zhou et al. (2018) studied the heat wave in 2017 in the Yangtze River Delta and concluded that the UHI could explain 58% of the record-breaking heat stress. Perkins (2015) reviewed previous studies on heat waves and noted that UHIs not only intensified heat stress on the first day but also weakened the ability of humans in urban areas to handle heat stress on the following day.

Although a positive interaction between UHIs and heat waves has been demonstrated in several regions, different results were also observed in cities under different local background climates. Basara et al. (2010) studied the heat wave that occurred in 2008 in Oklahoma City and observed that the increase in UHI was stronger during the nighttime than during the daytime. However, McGregor et al. (2007) reported that only nighttime UHIs were intensified during the 2013 heat wave in London. Liao et al. (2018) studied the heat waves in China from 1961 to 2014 and concluded that the contribution of urbanization to heat waves was stronger under a wet background climate. Furthermore, Zhao, Oppenheimer, et al. (2018) studied UHIs during heat waves in the United States and identified that the interaction between UHIs and heat waves was significant in temperate climate areas but nonsignificant in dry regions.

The inconsistent interaction between UHIs and heat waves led researchers to investigate how UHIs perform differently during heat wave periods under different local background climates because local background climates have been demonstrated to strongly contribute to UHIs (Zhao et al., 2014) and heat waves (Yoon et al., 2018). As three megacities in China, Beijing, Shanghai, and Guangzhou are selected to represent typical cities under different local background climates, that is, temperate semihumid monsoon climate, subtropical humid monsoon climate, and marine subtropical monsoon climate, respectively (see Table 1). These three highly populated cities were all severely affected by heat waves and have experienced a series of problems related to heat-related illness, mortality, and power supply (Gao et al., 2015; Huang et al., 2010; Yang et al., 2013). This research aims to study the interaction between UHIs and heat waves in three megacities in China under different local background climates. In addition, the apparent temperature (AT, also called the human-perceived temperature), which represents the combined effects of temperature and humidity (Steadman, 1979), is also analyzed in this study to determine the impacts of different humidity conditions

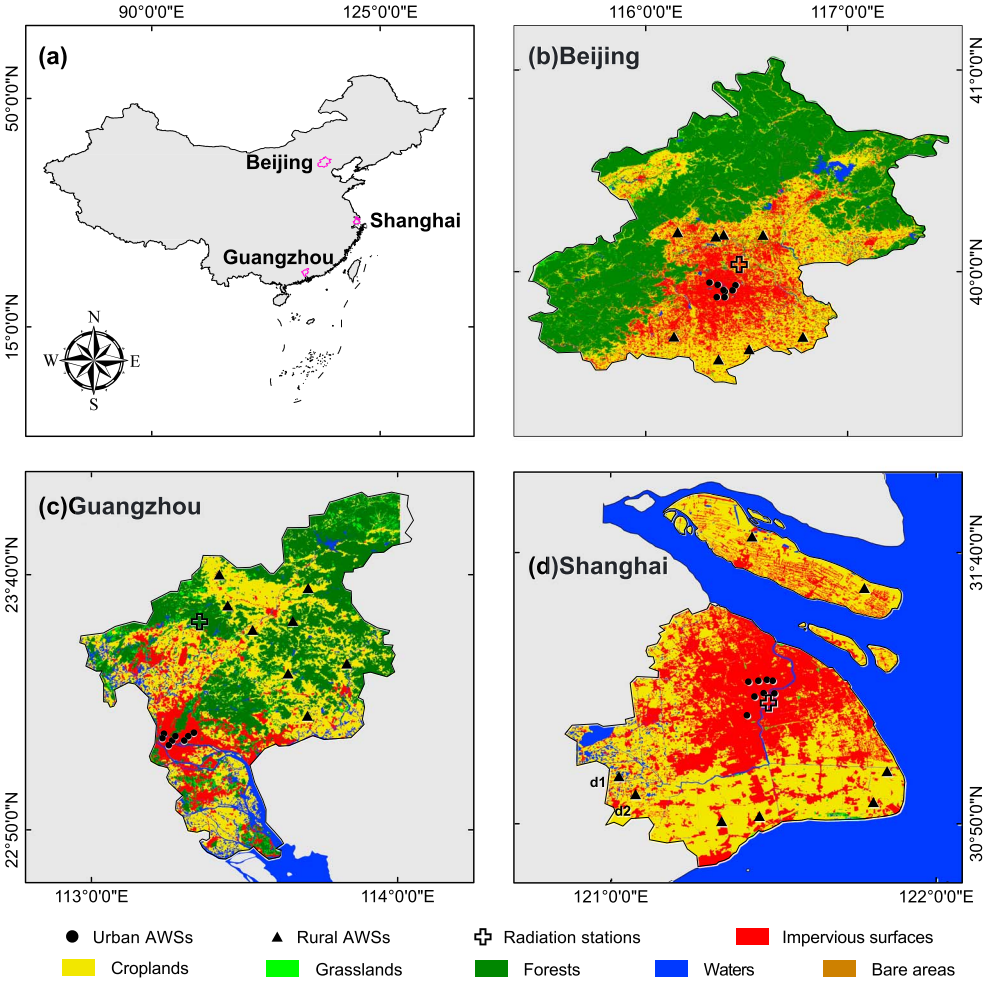

Figure 1. (a) Locations of Beijing, Shanghai, and Guangzhou and (b–d) the land cover types of Beijing, Shanghai, and Guangzhou in 2013. The urban automatic weather stations (AWSs), rural AWSs, and radiation stations are represented by different symbols. The two triangles d1 and d2 are two inland rural stations in Shanghai (Figure 1d), the remaining six rural stations are all coastal rural stations.

on humans (see section 3), because high relative humidity (RH) will put more heat stress on the human body under heat waves (Fischer & Schär, 2010).

2. Data and Methods

2.1. Data and Study Area

Beijing, Shanghai, and Guangzhou are the three largest megacities in China, and all three have sizable urban planning areas with high population pressure; however, these cities have different local background climates (Table 1). According to the Chinese National Bureau of Statistics, Beijing had a permanent resident population of 21.71 million in 2015, and the populations in Shanghai and Guangzhou had reached 24.15 million and 13.50 million, respectively (Table 1). Beijing experiences a typical north temperate semihumid continental monsoon climate, Shanghai experiences a subtropical humid monsoon climate, and Guangzhou experiences a marine subtropical monsoon climate. The western and northern parts of Beijing are surrounded by mountains, while the southeastern part of Shanghai is adjacent to the East China Sea, and the southern part of Guangzhou is close to the South China Sea (Figure 1). The sea-land breeze strongly impacts Shanghai due to its geographical location.

Ground-based hourly meteorological observations (including air temperature, wind speed, and wind direction) from 1 June to 31 August from 2013 to 2015 were collected from automatic weather stations (AWSs;

Figure 1) and obtained from the China Meteorological Administration to study UHIs during heat waves. The daily maximum temperatures in Shanghai and its neighboring cities during the study period were also collected. Surface solar radiation observations were collected at one radiation station in each city. Land cover type data in 2013 at 30-m resolution were used to calculate the percentages of different land cover types within a 1-km^2 circle around each station (Wang et al., 2017).

2.2. Methods Used to Evaluate UHIs Under Heat Waves/Normal Conditions

There are different definitions of heat waves, most of which are based on daily maximum or minimum temperature; the applied definition of a heat wave is generally depending on the study areas (Meehl & Tebaldi, 2004; Perkins, 2015; Robinson, 2001; Wang et al., 2015). According to the Chinese Meteorology Administration, a heat wave is defined as a period of at least three consecutive days with the daily maximum temperature (T_{max}) reaching 35 °C. The three studied cities are all located in China; therefore, we selected this definition in this study. In each city, all days when the daily T_{max} reached 35 °C in at least one urban station and lasted for more than 3 days were defined as heat waves; other days from 1 June to 31 August were defined as normal conditions. Therefore, considering the impact of weather conditions on the comparison of UHIs between heat waves and normal conditions, precipitation days (daily precipitation > 0.1 mm) and typhoon days were excluded according to the weather reports from the Chinese Meteorology Administration (Du et al., 2017; Walsh & Chapman, 1998).

To reduce the impact of the ambient environment background on the observations at the AWSs, the urban stations were selected according to the following considerations (Wang et al., 2017): (1) Stations had to be in central urban areas with more than 70% impervious surfaces. (2) The percentage of vegetation had to be less than 20% (i.e., stations in large urban parks were not selected). In order to better compare UHIs between the three cities, cropland was selected as the rural reference in all three cities because cropland was the main rural type that the studied three cities shared. The rural stations were selected based on the following considerations (Wang et al., 2017): (1) The percentage of impervious surfaces around the stations had to be less than 30%, and the percentage of croplands had to be greater than 65%. (2) The differences in the surface elevations between rural stations and urban stations had to be less than 30 m. (3) The rural sites had to be outside major urban areas. The locations and the numbers of selected AWSs are shown in Figure 1 and Table 1, respectively. The percentage of impervious surfaces around the urban station (1 km^2) had a significant positive impact on UHIs, which had already been demonstrated in our previous study (Wang et al., 2017). Therefore, urban stations with a high percentage of impervious surfaces and rural stations with a low percentage of impervious surfaces were selected to reduce the impact of the station's surroundings. At last, in each city, we selected eight rural stations and eight urban stations, respectively.

The data from all rural AWSs were averaged to represent a typical rural station. The data collected at the urban AWSs were processed in the same way when investigating the diurnal variations in air temperatures (T_a) and AT (Figures 2a1–2a3 and 6a1–6a3). UHIs at each urban station were calculated; afterward, UHIs at all urban stations were averaged to represent the averaged UHI (Figures 2b1–2b3 and 7b1–7b3). Similarly, the data under heat waves/normal conditions were averaged to compare the results under different conditions. When analyzing the correlation between UHIs and solar radiation (Figure 4), the independent data series from each day was used. Other elements, that is, RH and wind speed, were processed in the same way. Also, the averages from 10:00 to 16:00 and from 22:00 to 4:00 were used to represent daytime and nighttime averages, respectively (Wang et al., 2017). The T_{max} anomalies collected at ~220 stations during a heat wave period (8 to 12 July 2013) in Shanghai, and its neighboring cities were used in Figure 6. Each pixel represents a 0.2° × 0.2° grid cell; 98% of the pixels have values that contain only one station, and the remaining pixels (2%) have values that represent the average of the T_{max} observed at two contained stations.

The method used to calculate the average wind speed/wind direction was the same as that used by NOAA (https://www.ndbc.noaa.gov/wndav.shtml). The simple average of the wind speed observations was regarded as the average wind speed. The average wind direction was a “unit-vector” average. To obtain the main wind direction, the outliers in the wind direction data were excluded. For each set of wind direction data during daytime/nighttime at each station, when the difference between one wind direction and the averaged daytime/nighttime wind direction was larger than two times of the standard deviation of the set of wind directions (Miller, 1991), these wind direction data and their related wind speed data were

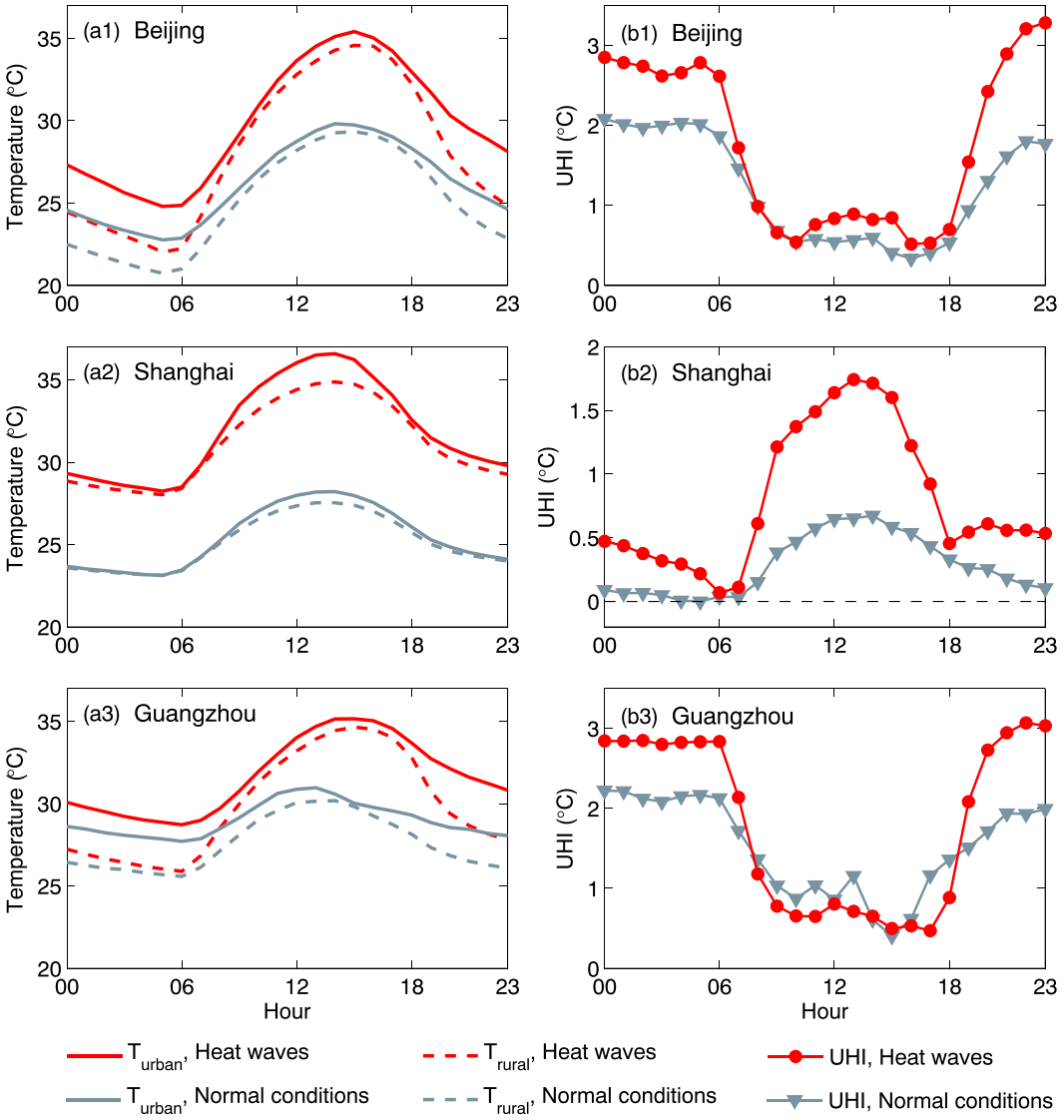

Figure 2. Time series of (a1–a3) hourly air temperatures (T_a) and (b1–b3) hourly urban heat islands (UHIs) in Beijing, Shanghai, and Guangzhou under heat waves/normal conditions. Red lines denote the results under heat waves, and gray lines denote the results under normal conditions.

removed. The wind data collected at all urban and rural stations were used in Figure 5 since the wind directions in urban areas and rural areas were relatively consistent according to the ground observations.

To better compare the impact of heat waves on the human body, AT (https://www.wpc.ncep.noaa.gov/html/heatindex_equation.shtml?tdsourcetag=s_pcqq_aiomsg) and its related apparent UHIs (UHIs derived from AT) were also analyzed in these three cities. The AT is calculated by using the full Rothfusz regression and including adjustments (Rothfusz, 1990). The same data processing method used in Figure 2 was applied to Figure 7 to analyze the diurnal cycles of AT and apparent UHIs.

3. Results

3.1. Amplified UHIs Under Heat Waves

Figures 2a1–2a3 displays the diurnal variations in the averaged T_a under heat waves and normal conditions in Beijing, Shanghai, and Guangzhou. The T_a values were higher in urban areas than in rural areas in all three cities, regardless of heat waves or normal conditions (Figures 2a1–2a3). During heat waves, diurnal

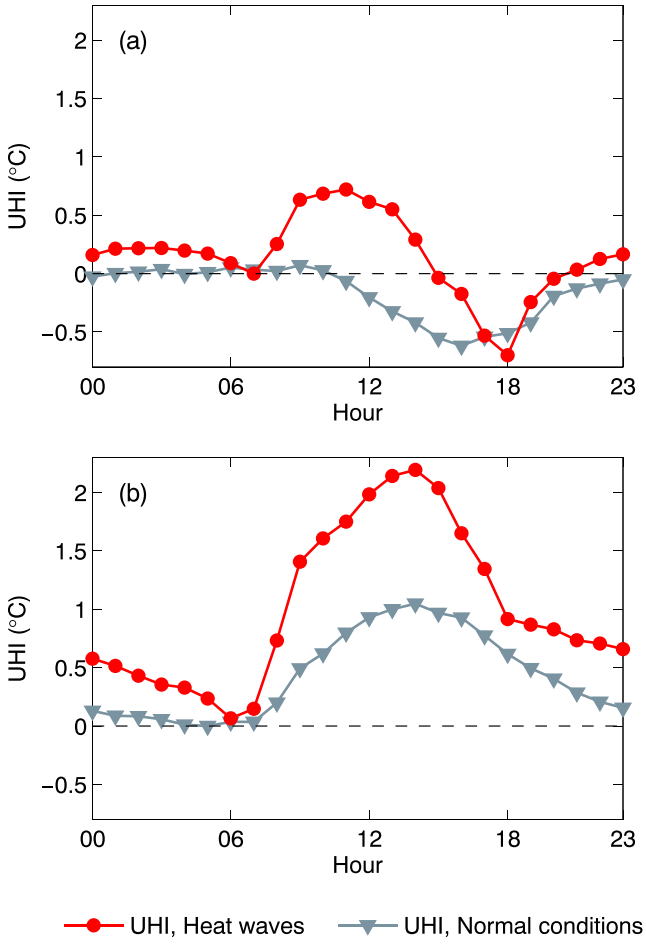

Figure 3. Time series of hourly urban heat islands (UHIs) in Shanghai using different rural reference. (a) The two inland rural stations (d1 and d2, in Figure 1d) were selected as the rural reference, whereas (b) the remaining six coastal rural stations (in Figure 1d) were selected as the rural reference. Red lines denote the results under heat waves, and gray lines denote the results under normal conditions.

temperature range decreases from 10.6 ± 0.64 °C (mean ± 1 standard deviation) in Beijing to 8.3 ± 0.42 °C in Shanghai and 6.4 ± 0.56 °C in Guangzhou with the background climate varying from temperate semihumid monsoon to subtropical humid monsoon and marine subtropical monsoon. However, the three cities have similar T_{max} during heat waves and normal conditions.

The diurnal cycles of UHIs under heat waves and normal conditions are shown in Figures 2b1–2b3. In spite of the fact that Beijing and Guangzhou have the largest contrast in background climate, they shared similar diurnal cycles of UHIs, that is, weak UHIs during daytime and strong UHIs during nighttime (Figures 2b1 and 2b3). However, UHIs in Shanghai showed a contrary diurnal cycle, that is, strong UHIs during daytime and weak UHIs during nighttime (Figure 2b2). This phenomenon was observed because the mean and diurnal cycle of UHI was significantly depending on the selection of rural reference stations. When using two inland rural stations as the reference, UHIs in Shanghai were much less but showed similar diurnal cycles to those in Beijing and Guangzhou. A more interesting finding is that UHIs were negative during the afternoon in Shanghai (Figure 3a) when referenced to inland rural stations; the negative daytime UHIs had also been reported in Beijing (Wang et al., 2007; Wang et al., 2017). However, if the six coastal cropland stations were selected as rural reference stations, strong daytime UHIs were observed in Shanghai under both heat waves and normal conditions (Figure 3b). This difference was observed because rural coastal stations were extensively impacted by the land-sea breeze. Similar results had been reported elsewhere (Tan et al., 2008). These diurnal cycles of UHIs in Beijing, Shanghai, and Guangzhou were consistent with the cycles found in previous studies (Huang et al., 2010; Meng et al., 2011; Wang et al., 2017).

The comparison of UHIs under heat waves and normal conditions also shows a different result. Although UHIs were stronger for most hours under heat waves than under normal conditions in all three cities, Beijing and Guangzhou tended to exhibit higher nighttime UHI_{max} (3.3 ± 0.80 and 3.1 ± 0.23 °C, respectively) and greater diurnal UHI ranges (2.8 ± 0.70 and 2.6 ± 0.44 °C, respectively) under heat waves than under normal conditions, whereas Shanghai exhibited a stronger daytime UHI_{max} (1.7 ± 0.44 °C) under heat waves than under normal conditions (see Table 2). Nighttime UHIs (averaged from 22:00 to 04:00) under heat waves in Beijing and Guangzhou were amplified by 0.9 ± 0.36 and 0.8 ± 0.20 °C, respectively. The daytime UHI (averaged from 10:00 to 16:00) in Shanghai was amplified by 0.9 ± 0.13 °C under heat weaves.

3.2. Strong Contributions of Solar Radiation to UHIs Under Heat Waves

Solar radiation was analyzed to better understand the heat stress resulting from solar energy (Figure 4). The surface solar radiation (daily total solar radiation) was approximately 1.5 times stronger under heat waves than under normal conditions (Figures 4a3, 4b3, and 4c3) in all three cities. This result indicates that days under heat waves tend to have less cloud and permits more solar radiation reaching the surface (De Boeck et al., 2010; Ding et al., 2010), which in turn amplifies the heat stress under heat waves (Hathway & Sharples, 2012). In this study, we go further to show that the enhanced surface solar radiation during heat wave period also increases the UHI.

The correlations between daily total solar radiation and UHIs during daytime and nighttime were both analyzed (Figures 4a1, 4a2, 4b1, 4b2, 4c1, and 4c2). A significant correlation was observed between UHIs and solar radiation in Beijing during the nighttime, which was stronger under heat waves ($r = 0.76$, $p < 0.01$) than that under normal conditions ($r = 0.31$, $p < 0.01$). For Shanghai, daytime UHIs were significantly

Table 2
The T_{max}, DTR, and UHIs (Mean ± 1 Standard Deviation) Derived From T_a and AT Under Heat Waves and Normal Conditions in Beijing, Shanghai, and Guangzhou (°C)

Temperature		Conditions	Beijing	Shanghai	Guangzhou
T_a	Daily urban T_{max}	Heat waves	35.4 ± 0.51	36.6 ± 0.38	35.2 ± 0.55
		Normal conditions	29.8 ± 0.45	28.2 ± 0.33	31.0 ± 0.35
	Daily DTR	Heat waves	10.6 ± 0.64	8.3 ± 0.42	6.4 ± 0.56
		Normal conditions	7.1 ± 0.48	5.0 ± 0.46	3.3 ± 0.34
	Daily UHI_{max}	Heat waves	3.3 ± 0.80	1.7 ± 0.44	3.1 ± 0.23
		Normal conditions	2.1 ± 0.45	0.7 ± 0.33	2.2 ± 0.18
	Diurnal UHI range	Heat waves	2.8 ± 0.70	1.7 ± 0.41	2.6 ± 0.44
		Normal conditions	1.7 ± 0.39	0.7 ± 0.36	1.8 ± 0.14
	Daytime UHI	Heat waves	0.7 ± 0.15	1.5 ± 0.18	0.6 ± 0.10
		Normal conditions	0.5 ± 0.09	0.6 ± 0.07	0.8 ± 0.26
	Nighttime UHI	Heat waves	2.9 ± 0.26	0.4 ± 0.10	2.9 ± 0.10
		Normal conditions	2.0 ± 0.11	0.1 ± 0.04	2.1 ± 0.10
AT	Daily urban AT_{max}	Heat waves	36.0 ± 0.94	49.2 ± 1.28	33.7 ± 1.05
		Normal conditions	30.9 ± 0.65	32.1 ± 0.70	30.6 ± 0.70
	Daily DTR	Heat waves	10.6 ± 1.06	15.6 ± 1.53	5.3 ± 1.04
		Normal conditions	7.7 ± 0.70	7.5 ± 0.90	3.1 ± 0.82
	Daily UHI_{max}	Heat waves	3.4 ± 0.72	5.3 ± 0.76	3.6 ± 0.53
		Normal conditions	2.2 ± 0.40	1.4 ± 0.25	2.9 ± 0.44
	Diurnal UHI range	Heat waves	3.5 ± 0.62	5.1 ± 0.82	2.5 ± 0.57
		Normal conditions	2.0 ± 0.57	1.4 ± 0.42	2.0 ± 0.47
	Daytime UHI	Heat waves	0.2 ± 0.23	4.7 ± 0.42	1.4 ± 0.18
		Normal conditions	0.3 ± 0.08	1.3 ± 0.11	1.6 ± 0.41
	Nighttime UHI	Heat waves	3.2 ± 0.23	1.5 ± 0.52	3.3 ± 0.19
		Normal conditions	2.0 ± 0.08	0.2 ± 0.08	2.8 ± 0.18

Note. The calculated standard deviation represents the interstation difference. The averages from 10:00 to 16:00 and from 22:00 to 4:00 were used to represent daytime and nighttime averages, respectively. AT = apparent temperature; DTR = diurnal temperature range; UHI = urban heat island.

correlated with solar radiation under both heat waves ($r = 0.62$, $p < 0.01$) and normal conditions ($r = 0.67$, $p < 0.01$). Nighttime UHIs were significantly correlated with solar radiation under heat waves in Guangzhou ($r = 0.30$, $p < 0.01$). However, no significant correlation was found between solar radiation and nighttime UHIs in Shanghai, and the correlations between daytime UHIs and solar radiation in Beijing and Guangzhou were insignificant either. Compared to nighttime UHIs (2.9 ± 0.26 and 2.9 ± 0.10 °C, respectively), daytime UHIs (0.7 ± 0.15 and 0.6 ± 0.10 °C, respectively) in Beijing and Guangzhou were very weak throughout the study period. The low signal-to-noise ratio of the UHIs may be the reason for the low correlations.

3.3. Changes in Wind Direction Under Heat Waves in Shanghai

The wind roses in Beijing, Shanghai, and Guangzhou under heat waves and normal conditions are shown in Figure 5. The wind directions during daytime and nighttime were consistent under heat waves and normal conditions in Beijing and Guangzhou (Figures 5a1–5a4 and 5c1–5c4; the principal wind direction: south-southeast). However, the daytime wind direction in Shanghai differed between heat waves and normal conditions. The principal daytime wind direction was southwest (more than 63% of the wind direction; Figure 5b1) under heat waves but was southeast (more than 70% of the wind direction; Figure 5b2) under normal conditions.

Due to the impact of wind direction changes, air temperature in neighboring cities may have an impact on the daytime heat stress in Shanghai. Figure 6 shows the T_{max} anomaly in Shanghai and its neighbor cities during a heat wave period (from 8 to 12 July 2013). The T_{max} anomaly in eastern neighboring cities (e.g., Shanghai and northern Zhejiang) began to increase before the occurrence of the heat wave in Shanghai (Figures 6a1–6a3); these high temperature anomalies then moved westward (Figures 6a4–6a6). After the heat wave ending (Figures 6a7–6a9), high T_{max} anomalies moved continually westward and disappeared from this area. Previous studies also showed that heat waves in the Yangtze River Delta, especially Shanghai, and many parts of southern China are triggered by the western Pacific subtropical high, and their

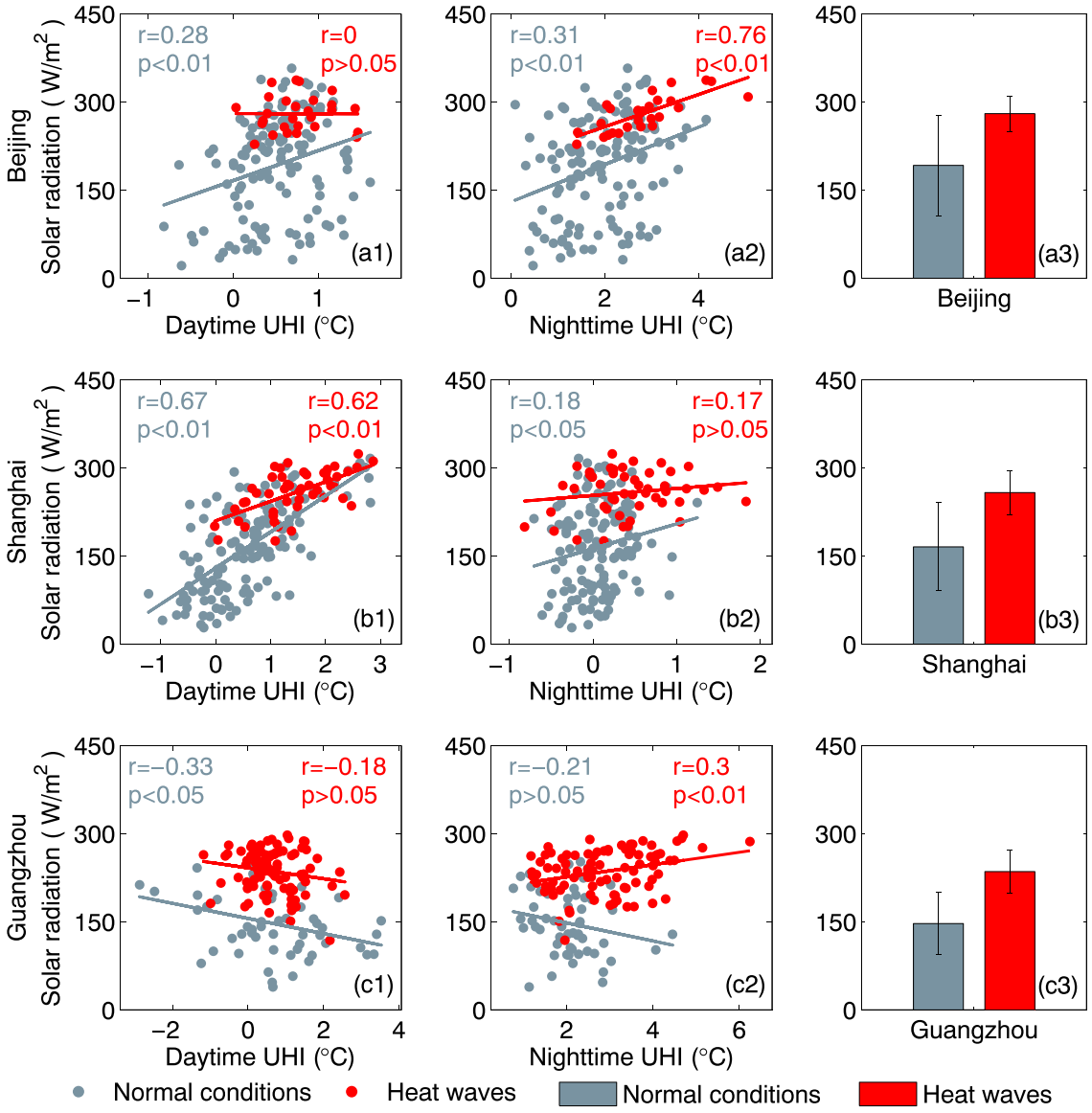

Figure 4. Scatterplots of daily total solar radiation as a function of daytime/nighttime urban heat islands (UHIs) in (a1, a2) Beijing, (b1, b2) Shanghai, and (c1, c2) Guangzhou. (a3, b3, c3) The average values (bars) and the standard deviations (whiskers) of solar radiation under heat waves/normal conditions. Red symbols denote the result under heat waves, gray symbols denote the results under normal conditions.

air temperatures also begin to increase in the east and then move westward (Ding et al., 2010; Luo & Lau, 2017; Wang et al., 2014), which makes more wind come from neighboring hot cities in the southwest rather than from the cool sea areas in the southeast.

3.4. Amplified Apparent UHIs Under Heat Waves

Figures 7a1–7a3 show the diurnal cycles of AT under heat waves and normal conditions. Nighttime AT was higher under heat waves than under normal conditions in Beijing and Guangzhou, and daytime AT was higher under heat waves than under normal conditions in Shanghai. Compared to Beijing and Guangzhou, Shanghai had a very high daytime AT_{max} (49.2 ± 1.28 °C) and a large diurnal AT range (15.6 ± 1.53 °C) under heat waves. Guangzhou had a lower daily AT_{max} (33.9 ± 1.05 °C) and a lower diurnal AT range (5.4 ± 1.04 °C) under heat waves than had Beijing (AT_{max}: 36 ± 0.94 °C, diurnal AT range: 10.6 ± 1.06 °C).

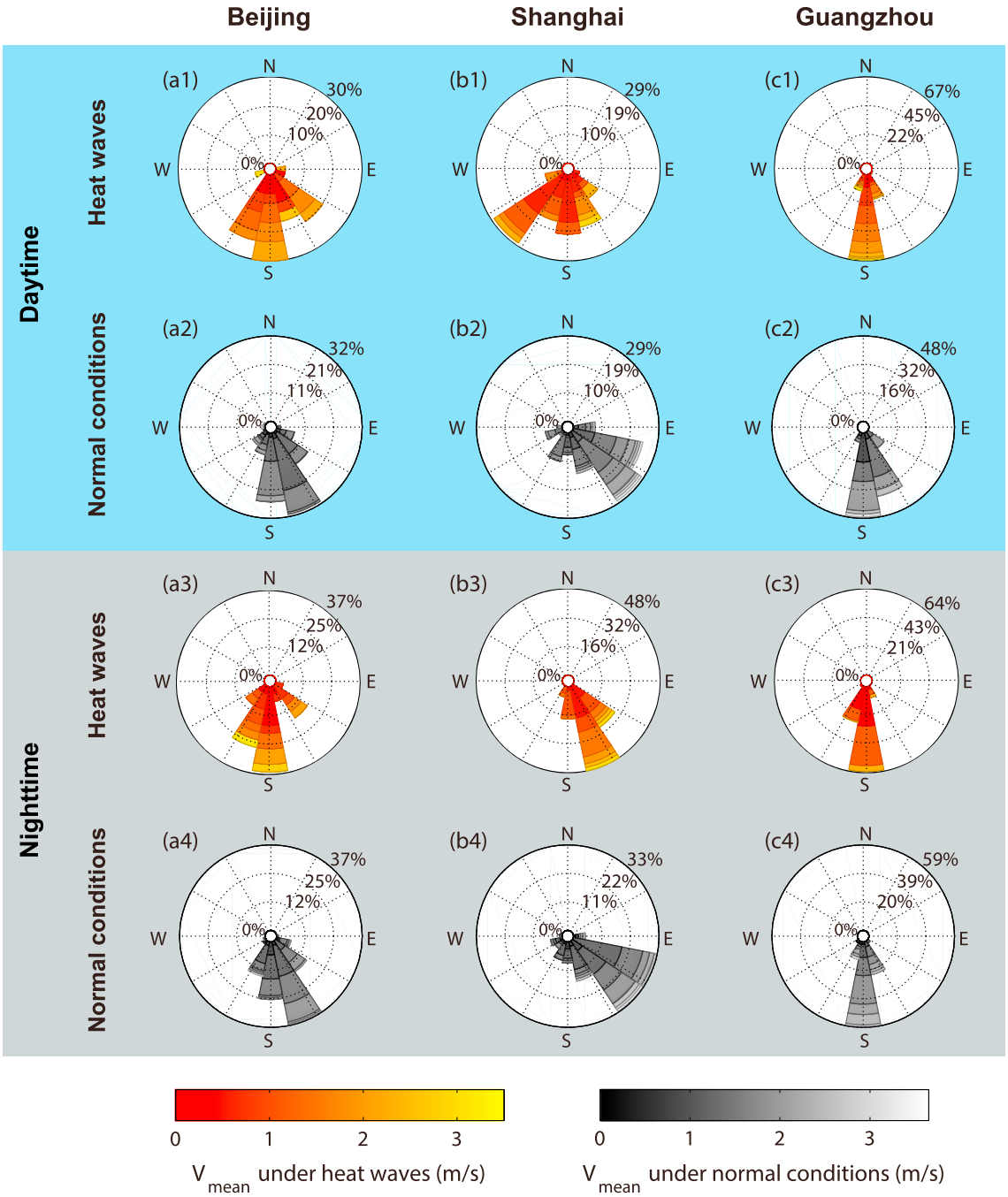

Figure 5. Wind roses in Beijing, Shanghai, and Guangzhou during daytime/nighttime: (a2, b2, c2, a4, b4, and c4) under normal conditions and (a1, b1, c1, a3, b3, and c3) under heat waves.

Figures 7b1–7b3 show the diurnal cycles of apparent UHIs (UHIs derived from AT). Nighttime apparent UHIs were stronger under heat waves than under normal conditions in all three cities, and daytime apparent UHIs were stronger under heat waves than under normal conditions in Shanghai. Beijing and Guangzhou exhibited stronger nighttime apparent UHIs (3.2 ± 0.23 and 3.6 ± 0.19 °C, respectively; see Table 2) under heat waves than under normal conditions (2.0 ± 0.08 and 2.9 ± 0.18 °C, respectively). Shanghai had a stronger daytime apparent UHI under heat waves (4.6 ± 0.42 °C) than under normal conditions (1.5 ± 0.11 °C). The diurnal apparent UHI range was larger in Shanghai (4.9 ± 0.82 °C) under heat waves than in Beijing and Guangzhou (3.5 ± 0.62 and 2.6 ± 0.57 °C, respectively).

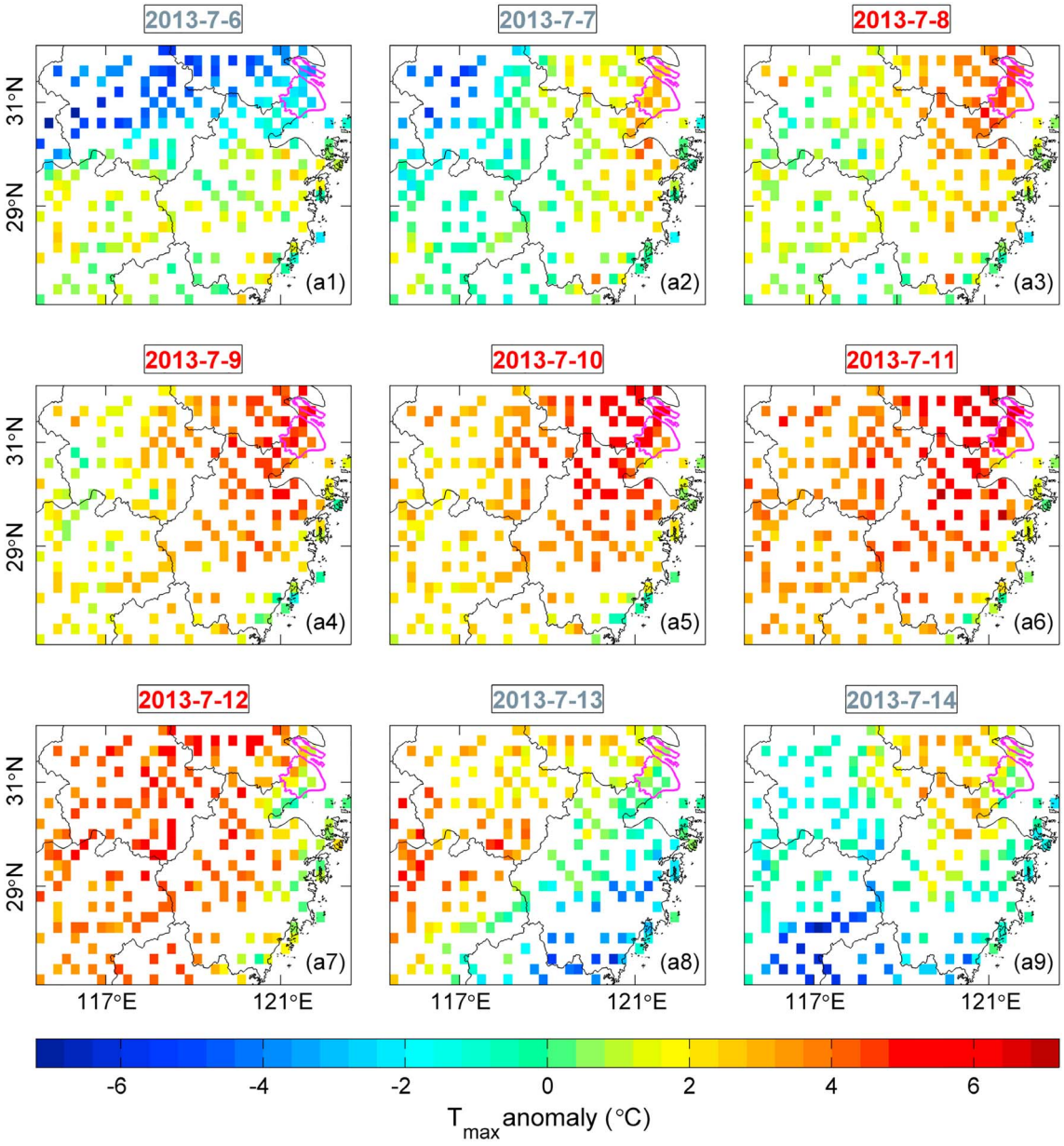

Figure 6. The T_{max} anomalies during (a3–a7) a heat wave period (8 to 12 July 2013) and (a1, a2, a8, a9) normal conditions in Shanghai and its neighboring cities. The area with pink border lines is Shanghai. The averaged T_{max} during the period July 1986–2015 was used as a reference to calculate the T_{max} anomaly.

Apparent UHIs were calculated based on air temperature and RH. Figure 8 shows the diurnal cycles of RH and the urban-rural difference in RH ($RH_{urban\text{-}rural}$). The RH under heat waves were lower than that under normal conditions for most hours in all three cities. This phenomenon is also called the urban dry island, which can be intensified by urban expansion as well (Hao et al., 2018; Luo & Lau, 2019; Yang, Ren, et al., 2017). The RH in Shanghai was higher than that in Beijing and Guangzhou, which could explain the highest AT in Shanghai. The strong urban-rural RH contrasts in Beijing led to a significant correlation between $RH_{urban\text{-}rural}$ and UHIs (Figure 9) during both daytime ($r = -0.62$, $p < 0.01$) and nighttime ($r = -0.73$, $p < 0.01$) under heat waves, the significant correlations were also observed under normal conditions in Beijing. However, the $RH_{urban\text{-}rural}$ in Shanghai was not significantly related to UHIs, and the correlation between $RH_{urban\text{-}rural}$ and UHIs was also low in Guangzhou (Figure 9).

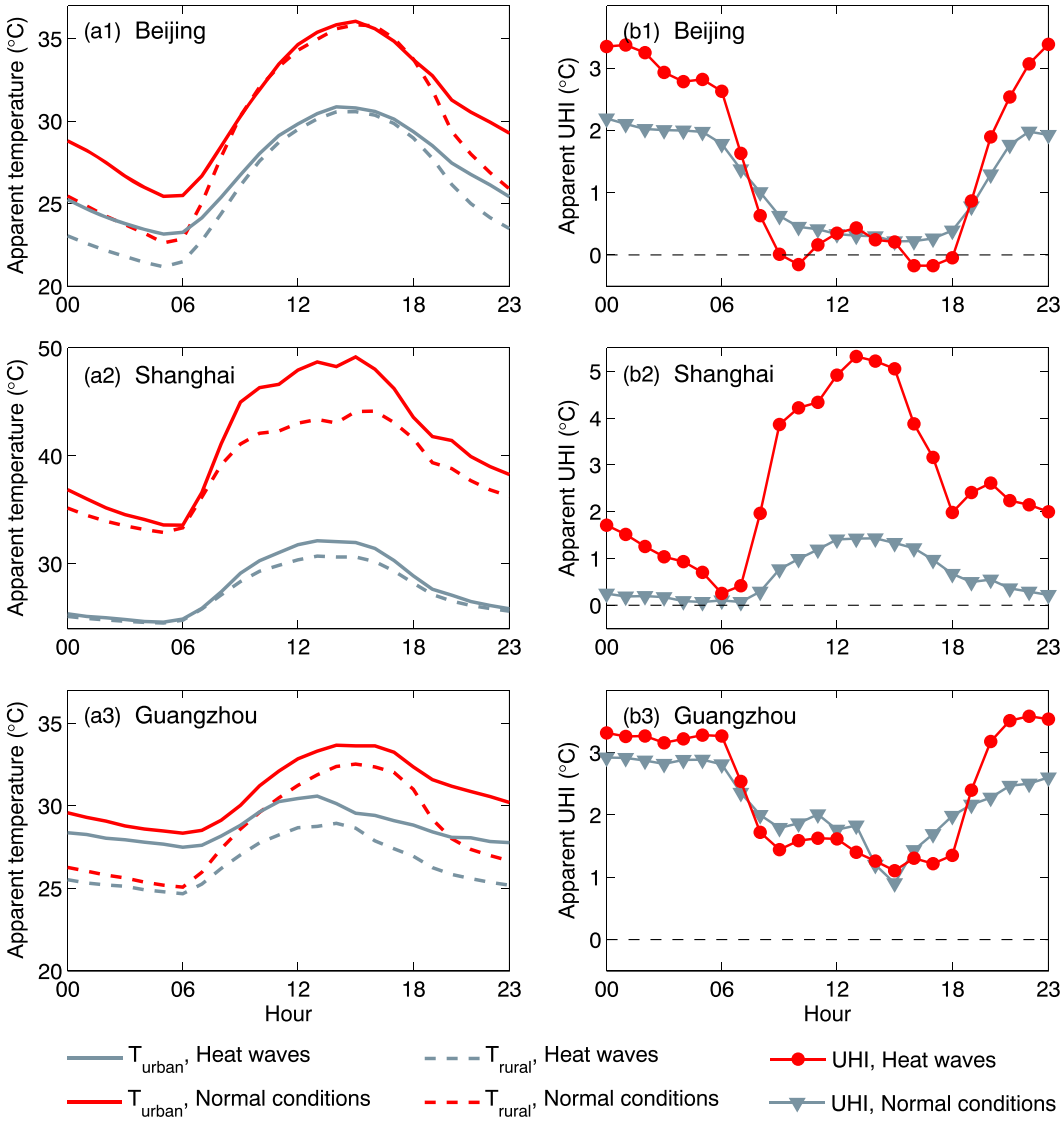

Figure 7. Time series of (a1–a3) hourly apparent temperature and (b1–b3) hourly apparent urban heat islands (UHIs) in Beijing, Shanghai, and Guangzhou under heat waves/normal conditions. Red lines denote the results under heat waves, and gray lines denote the results under normal conditions.

4. Discussion

This study shows that the surface solar radiation during heat wave period is generally higher under heat waves than that under normal conditions. This is because heat waves generally come with a high-pressure system (e.g., western Pacific subtropical high) and less cloud compared with normal conditions (De Boeck et al., 2010; Ding et al., 2010; Luo & Lau, 2017). The enhanced surface solar radiation in turn increases the air temperature under heat waves. Moreover, the T_a in rural areas tended to increase faster; this phenomenon was most likely due to urban geometry, which was often understood to be the cause (Oke, 1981). Observations and model simulations have demonstrated that the surface solar radiation was intercepted and deposited in the urban canopy during daytime and released during nighttime, which is an important factor determining UHIs (Liu et al., 2014; Oke, 1981; Wang et al., 2017). This impact does not change with the local climate. Therefore, Beijing and Guangzhou showed similar characteristics in the interaction between heat waves and UHIs. Similar results were observed in other inland cities. For example, nighttime UHIs were demonstrated to be strongly intensified in Oklahoma (an inland city) under heat waves (Basara et al., 2010).

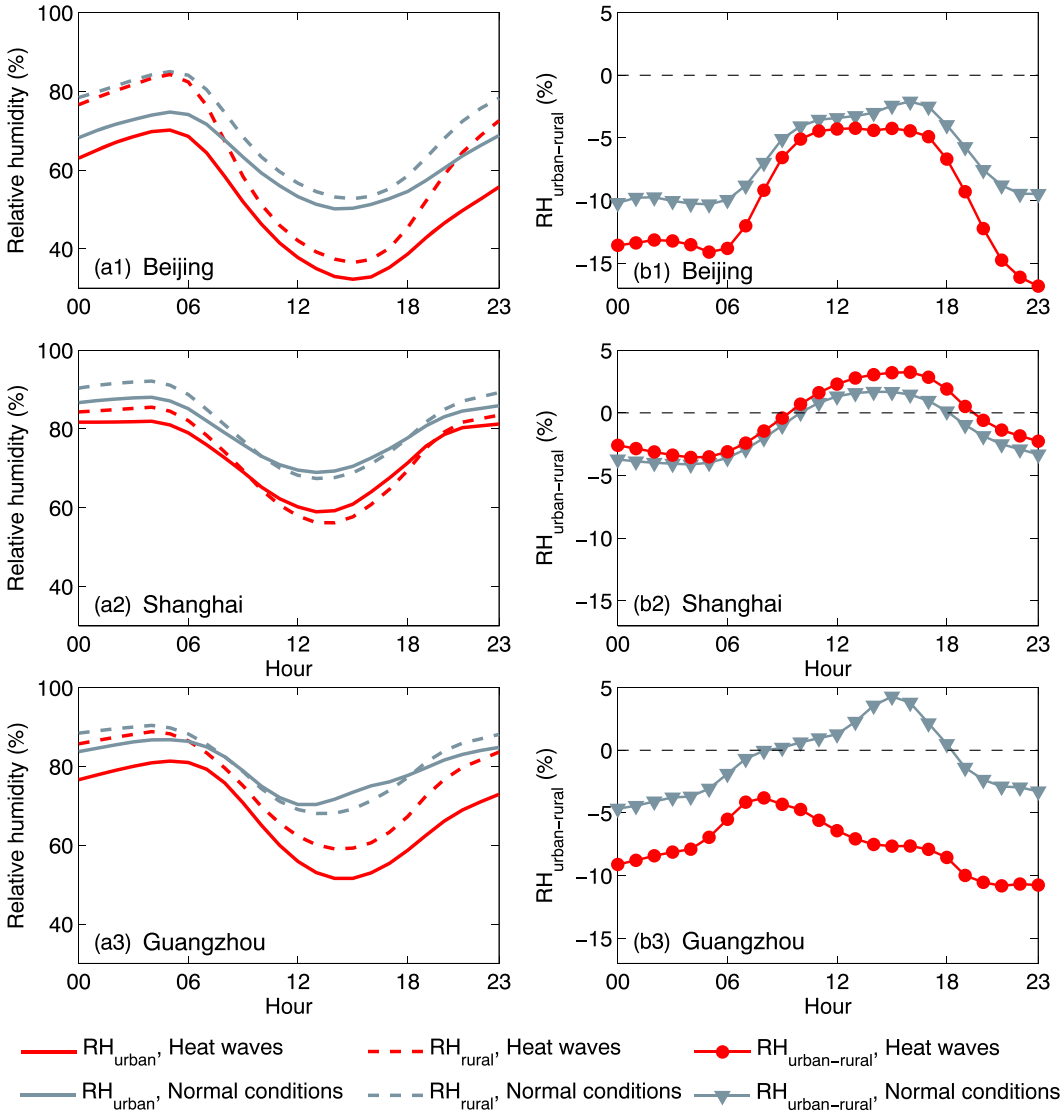

Figure 8. Time series of (a1–a3) hourly relative humidity (RH) and (b1–b3) hourly urban-rural difference in relative humidity ($RH_{urban-rural}$) in Beijing, Shanghai, and Guangzhou under heat waves/normal conditions. Red lines denote the results under heat waves, and gray lines denote the results under normal conditions.

However, Shanghai is a coastal city, whose UHIs tend to be impacted by the land-sea breeze. UHIs in Shanghai were more obvious at daytime under heat waves if the coastal rural stations were selected as the rural reference (Figure 3b). Different principle wind directions were observed in Shanghai during the daytime, and the main daytime direction was southwest under heat waves but changed to southeast under normal conditions. On the one hand, with less wind originating from the cooler sea areas, the air temperatures in urban and rural areas were hotter at daytime under heat waves. On the other hand, more dry air from land came with less cloud, which permitted more solar radiation reaching the surface at daytime under heat waves (De Boeck et al., 2010; Ding et al., 2010). The enhanced surface solar radiation during heat wave period in turn increased the mean air temperature and the urban-rural contrast in air temperature (i.e., UHI). Similar results were observed in other coastal cities. For example, the intensified UHIs were stronger during daytime than during nighttime in Athen (a coastal city) under heat waves when referenced to three coastal rural stations (Founda & Santamouris, 2017).

Changes in wind speed had been demonstrated to have an important impact on UHIs in Beijing (Li et al., 2016). Li et al. (2016) studied the UHIs under heat waves in Beijing and observed enhanced urban wind speed during daytime and reduced urban wind speed during nighttime, which led to an enhanced UHI at

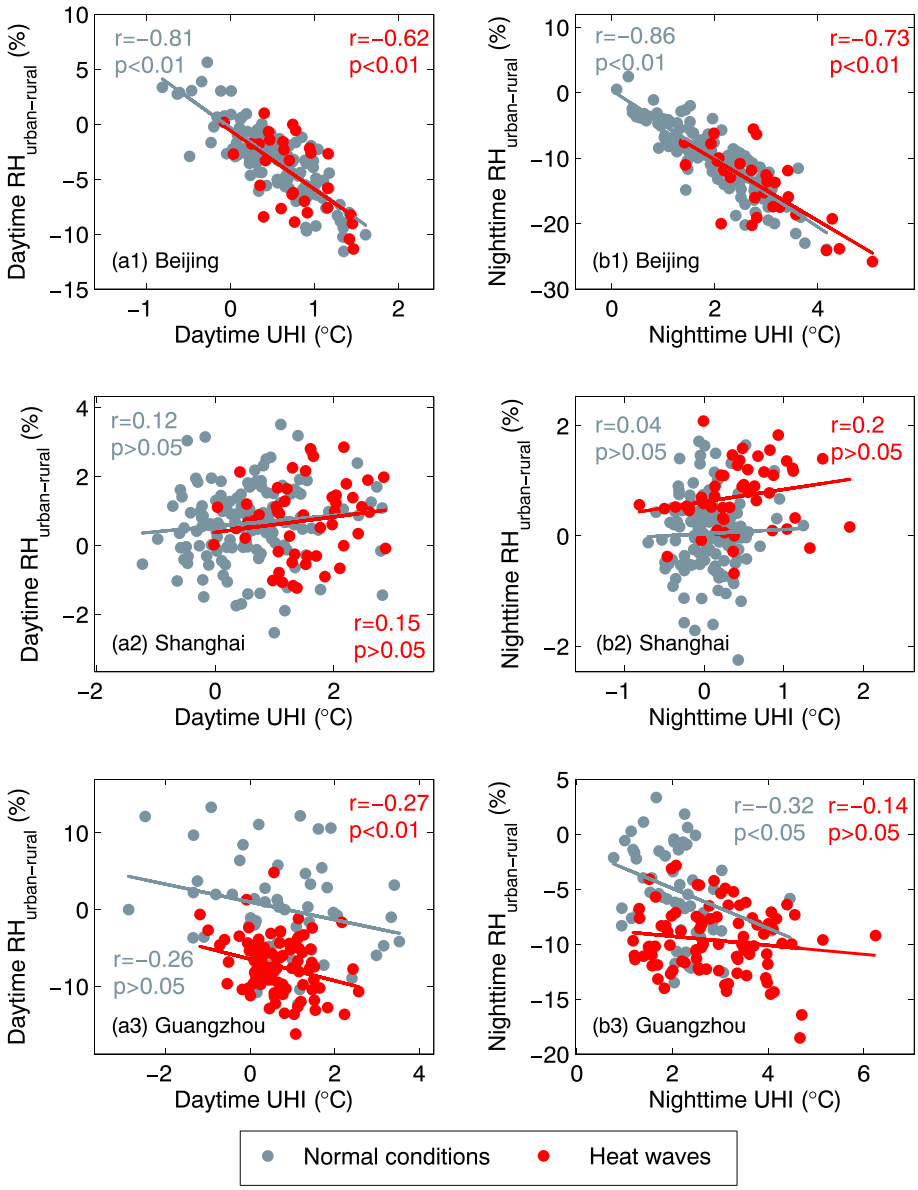

Figure 9. Scatterplots of urban-rural differences in relative humidity ($RH_{urban-rural}$) as a function of UHIs in (a1, a2) Beijing, (b1, b2) Shanghai, and (c1, c2) Guangzhou during daytime/nighttime. Red symbols denote the results under heat waves, gray symbols denote the results under normal conditions.

both daytime and nighttime. The positive correlation between $V_{urban-rural}$ (urban-rural wind speed difference) and UHIs were also observed at both daytime and nighttime in Beijing (Figures S2a1 and S2b1 in the supporting information). However, although there was strong urban-rural wind speed difference ($V_{urban-rural}$) in Shanghai (Figures S1a2 and S1b2), no significant correlations were observed between UHIs and $V_{urban-rural}$ in Shanghai (Figures S2a2 and S2b2). The correlations between UHIs and $V_{urban-rural}$ were also weak during heat waves in Guangzhou (Figures S2a3 and S2b3). In addition to these elements, increased anthropogenic heat use due to air conditioning (Smoyer-Tomic et al., 2003; Tan et al., 2007) may also contribute to intensification of UHIs under heat waves.

Nighttime AT was higher under heat waves than under normal conditions in Beijing and Guangzhou, whereas in Shanghai AT was higher for most hours of the day under heat waves than normal conditions. With a high daytime T_a and a high RH, Shanghai tended to have higher AT and stronger apparent UHIs during the daytime under heat waves than did Beijing and Guangzhou, which led to severe heat stress in urban

areas. Beijing tended to have strong apparent UHIs during nighttime and weak apparent UHIs during daytime. Guangzhou tended to have stronger apparent UHIs during nighttime than during daytime.

5. Conclusion

Atmospheric UHIs under heat waves/normal conditions were compared in different local background climates. Although located under different local background climates, Beijing and Guangzhou tended to have similar diurnal cycles of UHIs, which were strong during nighttime and weak during the daytime. Shanghai is impacted by the sea-land thermal difference and tends to exhibit strong daytime UHIs and weak nighttime UHIs. Solar radiation plays an important role in UHIs under heat waves. Solar radiation is significantly correlated with daytime UHIs in Shanghai and nighttime UHIs in Beijing and Guangzhou. The increased solar radiation under heat waves leads to a strong intensification of nighttime UHIs in Beijing and Guangzhou. Compared to UHIs under normal conditions, nighttime UHIs in Beijing and Guangzhou were intensified by 0.9 ± 0.36 and 0.8 ± 0.20 °C under heat waves, respectively, and daytime UHIs in Shanghai were intensified by 0.9 ± 0.13 °C under heat waves.

The heat stress brought by the intensified UHIs would pose a severe threat to life and health of human during heat waves. According to Anderson and Bell (2011), the heat-related mortality risk would increase by 2.49% for every 0.55 °C increase during heat wave periods. Besides, changes in wind direction also contributed to the strong daytime UHIs in Shanghai under heat waves. In addition to solar radiation and wind, other synoptic conditions, such as increased surface pressure, reduced cloud cover, decreased precipitation, advective moisture, and drier air column over the area, may also contribute to heat waves (Lau & Nath, 2014; Luo & Lau, 2017; Wang, Zhou, et al., 2016), which may have an impact on UHIs in the three cities under heat waves and need further studies.

Acknowledgments
This study was funded by the National Key R&D Program of China (2017YFA0603601) and the National Natural Science Foundation of China (41525018). The meteorological observations were obtained from the Chinese Meteorological Administration (http://data.cma.cn/data/). The land cover type data at 30-m resolution in 2013 were obtained from National Geomatics Center of China (http://glc30.tianditu.com/). The city data in Table 1 were obtained from Chinese National Bureau of Statistics (http://www.stats.gov.cn/tjsj/ndsj/).

References

Anderson, G. B., & Bell, M. L. (2011). Heat waves in the United States: Mortality risk during heat waves and effect modification by heat wave characteristics in 43 U.S. Communities. *Environmental Health Perspectives*, *119*(2), 210–218. https://doi.org/10.1289/ehp.1002313

Angel, S., Parent, J., Civco, D. L., Blei, A., & Potere, D. (2011). The dimensions of global urban expansion: Estimates and projections for all countries, 2000–2050. *Progress in Planning*, *75*(2), 53–107. https://doi.org/10.1016/j.progress.2011.04.001

Arnfield, A. J. (2003). Two decades of urban climate research: A review of turbulence, exchanges of energy and water, and the urban heat island. *International Journal of Climatology*, *23*(1), 1–26. https://doi.org/10.1002/joc.859

Basara, J. B., Basara, H. G., Illston, B. G., & Crawford, K. C. (2010). The impact of the urban heat island during an intense heat wave in Oklahoma City. *Advances in Meteorology*, *2010*, 1–10. https://doi.org/10.1155/2010/230365

De Boeck, H. J., Dreesen, F. E., Janssens, I. A., & Nijs, I. (2010). Climatic characteristics of heat waves and their simulation in plant experiments. *Global Change Biology*, *16*(7), 1992–2000. https://doi.org/10.1111/j.1365-2486.2009.02049.x

Ding, T., Qian, W., & Yan, Z. (2010). Changes in hot days and heat waves in China during 1961–2007. *International Journal of Climatology*, *30*, 1452–1462. https://doi.org/10.1002/joc.1989

Du, J., Wang, K., Wang, J., & Ma, Q. (2017). Contributions of surface solar radiation and precipitation to the spatiotemporal patterns of surface and air warming in China from 1960 to 2003. *Atmospheric Chemistry and Physics*, *17*(8), 4931–4944. https://doi.org/10.5194/acp-17-4931-2017

Fischer, E. M., & Schär, C. (2010). Consistent geographical patterns of changes in high-impact European heatwaves. *Nature Geoscience*, *3*(6), 398–403. https://doi.org/10.1038/ngeo866

Founda, D., & Santamouris, M. (2017). Synergies between urban heat island and heat waves in Athens (Greece), during an extremely hot summer (2012). *Scientific Reports*, *7*(1), 10973. https://doi.org/10.1038/s41598-017-11407-6

Gao, J., Sun, Y., Liu, Q., Zhou, M., Lu, Y., & Li, L. (2015). Impact of extreme high temperature on mortality and regional level definition of heat wave: A multi-city study in China. *Science of the Total Environment*, *505*, 535–544. https://doi.org/10.1016/j.scitotenv.2014.10.028

Hao, L., Huang, X., Qin, M., Liu, Y., Li, W., & Sun, G. (2018). Ecohydrological processes explain urban dry island effects in a wet region, southern China. *Water Resources Research*, *54*(9), 6757–6771. https://doi.org/10.1029/2018wr023002

Hathway, E. A., & Sharples, S. (2012). The interaction of rivers and urban form in mitigating the urban heat island effect: A UK case study. *Building and Environment*, *58*, 14–22. https://doi.org/10.1016/j.buildenv.2012.06.013

Huang, W., Kan, H., & Kovats, S. (2010). The impact of the 2003 heat wave on mortality in Shanghai, China. *Science of the Total Environment*, *408*(11), 2418–2420. https://doi.org/10.1016/j.scitotenv.2010.02.009

Ke, X., Wu, D., Rice, J., Kintner-Meyer, M., & Lu, N. (2016). Quantifying impacts of heat waves on power grid operation. *Applied Energy*, *183*, 504–512. https://doi.org/10.1016/j.apenergy.2016.08.188

Kovats, R. S., & Kristie, L. E. (2006). Heatwaves and public health in Europe. *European Journal of Public Health*, *16*(6), 592–599. https://doi.org/10.1093/eurpub/ckl049

Kuglitsch, F. G., Toreti, A., Xoplaki, E., Della-Marta, P. M., Zerefos, C. S., Türkeş, M., & Luterbacher, J. (2010). Heat wave changes in the eastern Mediterranean since 1960. *Geophysical Research Letters*, *37*, L04802. https://doi.org/10.1029/2009GL041841

Lau, N.-C., & Nath, M. J. (2014). Model Simulation and projection of European heat waves in present-day and future climates. *Journal of Climate*, *27*(10), 3713–3730. https://doi.org/10.1175/jcli-d-13-00284.1

Lewis, S. C., King, A. D., & Perkins-Kirkpatrick, S. E. (2017). Defining a new normal for extremes in a warming world. *Bulletin of the American Meteorological Society*, *98*(6), 1139–1151. https://doi.org/10.1175/bams-d-16-0183.1

Li, D., & Bou-Zeid, E. (2013). Synergistic Interactions between urban heat islands and heat waves: The impact in cities is larger than the sum of its parts. *Journal of Applied Meteorology and Climatology*, *52*(9), 2051–2064. https://doi.org/10.1175/jamc-d-13-02.1

Li, D., Sun, T., Liu, M., Wang, L., & Gao, Z. (2016). Changes in wind speed under heat waves enhance urban heat islands in the Beijing metropolitan area. *Journal of Applied Meteorology and Climatology*, *55*(11), 2369–2375. https://doi.org/10.1175/jamc-d-16-0102.1

Liao, W., Liu, X., Li, D., Luo, M., Wang, D., Wang, S., et al. (2018). Stronger contributions of urbanization to heat wave trends in wet climates. *Geophysical Research Letters*, *45*(20), 11,310–11,317. https://doi.org/10.1029/2018GL079679

Liu, Y., Xu, Y., & Ma, J. (2014). Quantitative assessment and planning simulation of Beijing urban heat island. *Ecology and Environmental Sciences*, *23*, 1156–1163.

Luo, M., & Lau, N.-C. (2017). Heat waves in southern China: Synoptic behavior, long-term change, and urbanization effects. *Journal of Climate*, *30*(2), 703–720. https://doi.org/10.1175/jcli-d-16-0269.1

Luo, M., & Lau, N.-C. (2018). Increasing heat stress in urban areas of eastern China: Acceleration by urbanization. *Geophysical Research Letters*, *45*(23), 13,060–13,069. https://doi.org/10.1029/2018GL080306

Luo, M., and N.-C. Lau2019: Urban expansion and drying climate in an urban agglomeration of east China. *Geophysical Research Letters*, *46*, 6868–6877. https://doi.org/10.1029/2019gl082736.

McGregor, G. R., Felling, M., Wolf, T., & Gosling, S. (2007). *The social impacts of heat waves*, (p. 41). Bristol, UK: Environment Agency.

Meehl, G. A., & Tebaldi, C. (2004). More intense, more frequent, and longer lasting heat waves in the 21st century. *Science*, *305*(5686), 994–997. https://doi.org/10.1126/science.1098704

Meng, W., Zhang, Y., Li, J., Lin, W., Dai, G., & Li, H. (2011). Application of WRF/UCM in the simulation of a heat wave event and urban heat island around Guangzhou. *Journal of Tropical Meteorology*, *17*, 256–265. https://doi.org/10.3969/j.issn.1006-8775.2011.03.007

Miller, J. (1991). Short report: Reaction time analysis with outlier exclusion: Bias varies with sample size. *The Quarterly Journal of Experimental Psychology Section A*, *43*(4), 907–912. https://doi.org/10.1080/14640749108400962

Oke, T. R. (1981). Canyon geometry and the nocturnal urban heat island: Comparison of scale model and field observations. *Journal of Climatology*, *1*(3), 237–254. https://doi.org/10.1002/joc.3370010304

Perkins, S. E. (2015). A review on the scientific understanding of heatwaves—Their measurement, driving mechanisms, and changes at the global scale. *Atmospheric Research*, *164-165*, 242–267. https://doi.org/10.1016/j.atmosres.2015.05.014

Poumadère, M., Mays, C., Le Mer, S., & Blong, R. (2005). The 2003 heat wave in France: Dangerous climate change here and now. *Risk Analysis*, *25*(6), 1483–1494. https://doi.org/10.1111/j.1539-6924.2005.00694.x

Robinson, P. J. (2001). On the definition of a heat wave. *Journal of Applied Meteorology*, *40*(4), 762–775. https://doi.org/10.1175/1520-0450(2001)040<0762:otdoah>2.0.co;2

Rothfusz, L. P. (1990). The heat index equation. In *National Weather Service Technical Attachment*, *Scientific Services Division NWS Southern Region Headquarters*, (pp. 90–23). TX, SR: Fort Worth.

Semenza, J. C., Rubin, C. H., Falter, K. H., Selanikio, J. D., Flanders, W. D., Howe, H. L., & Wilhelm, J. L. (1996). Heat-related deaths during the July 1995 heat wave in Chicago. *New England Journal of Medicine*, *335*(2), 84–90. https://doi.org/10.1056/nejm199607113350203

Smoyer-Tomic, K. E., Kuhn, R., & Hudson, A. (2003). Heat wave hazards: An overview of heat wave impacts in Canada. *Natural Hazards*, *28*(2/3), 465–486. https://doi.org/10.1023/a:1022946528157

Steadman, R. G. (1979). The assessment of sultriness. Part I: A temperature-humidity index based on human physiology and clothing science. *Journal of Applied Meteorology*, *18*(7), 861–873. https://doi.org/10.1175/1520-0450(1979)018<0861:taospi>2.0.co;2

Stewart, I. D., & Oke, T. R. (2012). Local climate zones for urban temperature studies. *Bulletin of the American Meteorological Society*, *93*(12), 1879–1900. https://doi.org/10.1175/bams-d-11-00019.1

Tan, J., Zheng, Y., Peng, L., Gu, S., & Shi, J. (2008). Effect of urban heat island on heat waves in summer of Shanghai. *Plateau meteorology*, *27*, 144–149.

Tan, J., Zheng, Y., Song, G., Kalkstein, L. S., Kalkstein, A. J., & Tang, X. (2007). Heat wave impacts on mortality in Shanghai, 1998 and 2003. *International Journal of Biometeorology*, *51*(3), 193–200. https://doi.org/10.1007/s00484-006-0058-3

United Nations (2014). In Population Division (Ed.), *World urbanization prospects: The 2014 version, highlights (ST/ESA/SER.A/352)*, (p. 32). New York: Department of Economic and Social Affairs.

Voogt, J. A., & Oke, T. R. (2003). Thermal remote sensing of urban climates. *Remote Sensing of Environment*, *86*(3), 370–384. https://doi.org/10.1016/s0034-4257(03)00079-8

Walsh, J. E., & Chapman, W. L. (1998). Arctic cloud–radiation–temperature associations in observational data and atmospheric reanalyses. *Journal of Climate*, *11*(11), 3030–3045. https://doi.org/10.1175/1520-0442(1998)011<3030:acrtai>2.0.co;2

Wang, J., Huang, B., Fu, D., Atkinson, P. M., & Zhang, X. (2016). Response of urban heat island to future urban expansion over the Beijing–Tianjin–Hebei metropolitan area. *Applied Geography*, *70*, 26–36. https://doi.org/10.1016/j.apgeog.2016.02.010

Wang, K., Jiang, S., Wang, J., Zhou, C., Wang, X., & Lee, X. (2017). Comparing the diurnal and seasonal variabilities of atmospheric and surface urban heat islands based on the Beijing urban meteorological network. *Journal of Geophysical Research: Atmospheres*, *122*, 2131–2154. https://doi.org/10.1002/2016JD025304

Wang, K., Wang, J., Wang, P., Sparrow, M., Yang, J., & Chen, H. (2007). Influences of urbanization on surface characteristics as derived from the Moderate-Resolution Imaging Spectroradiometer: A case study for the Beijing metropolitan area. *Journal of Geophysical Research*, *112*, D22S06. https://doi.org/10.1029/2006jd007997

Wang, W., Zhou, W., & Chen, D. (2014). Summer high temperature extremes in southeast China: Bonding with the El Niño–Southern Oscillation and East Asian summer monsoon coupled system. *Journal of Climate*, *27*(11), 4122–4138. https://doi.org/10.1175/jcli-d-13-00545.1

Wang, W., Zhou, W., Fong, S. K., Leong, K. C., Tang, I. M., Chang, S. W., & Leong, W. K. (2015). Extreme rainfall and summer heat waves in Macau based on statistical theory of extreme values. *Climate Research*, *66*(1), 91–101. https://doi.org/10.3354/cr01336

Wang, W., Zhou, W., Li, X., Wang, X., & Wang, D. (2016). Synoptic-scale characteristics and atmospheric controls of summer heat waves in China. *Climate Dynamics*, *46*(9-10), 2923–2941. https://doi.org/10.1007/s00382-015-2741-8

Wouters, H., De Ridder, K., Poelmans, L., Willems, P., Brouwers, J., Hosseinzadehtalaei, P., et al. (2017). Heat stress increase under climate change twice as large in cities as in rural areas: A study for a densely populated midlatitude maritime region. *Geophysical Research Letters*, *44*, 8997–9007. https://doi.org/10.1002/2017GL074889

Yang, J., Liu, H. Z., Ou, C. Q., Lin, G. Z., Ding, Y., Zhou, Q., et al. (2013). Impact of heat wave in 2005 on mortality in Guangzhou, China. *Biomedical and Environmental Sciences*, *26*(8), 647–654. https://doi.org/10.3967/0895-3988.2013.08.003

Yang, P., Ren, G., & Hou, W. (2017). Temporal–spatial patterns of relative humidity and the urban dryness island effect in Beijing city. *Journal of Applied Meteorology and Climatology*, *56*(8), 2221–2237. https://doi.org/10.1175/jamc-d-16-0338.1

Yang, X., Ruby Leung, L., Zhao, N., Zhao, C., Qian, Y., Hu, K., et al. (2017). Contribution of urbanization to the increase of extreme heat events in an urban agglomeration in east China. *Geophysical Research Letters*, *44*, 6940–6950. https://doi.org/10.1002/2017GL074084

Yoon, D., Cha, D.-H., Lee, G., Park, C., Lee, M.-I., & Min, K.-H. (2018). Impacts of synoptic and local factors on heat wave events over southeastern region of Korea in 2015. *Journal of Geophysical Research: Atmospheres*, *123*(21), 12,081–012,096. https://doi.org/10.1029/2018JD029247

Zhao, L. (2018). Urban growth and climate adaptation. *Nature Climate Change*, *8*(12), 1034–1034. https://doi.org/10.1038/s41558-018-0348-x

Zhao, L., Lee, X., Smith, R. B., & Oleson, K. (2014). Strong contributions of local background climate to urban heat islands. *Nature*, *511*(7508), 216–219. https://doi.org/10.1038/nature13462

Zhao, L., Oppenheimer, M., Zhu, Q., Baldwin, J. W., Ebi, K. L., Bou-Zeid, E., et al. (2018). Interactions between urban heat islands and heat waves. *Environmental Research Letters*, *13*(3), 034003. https://doi.org/10.1088/1748-9326/aa9f73

Zhou, C., Wang, K., Qi, D., & Tan, J. (2018). Attribution of a record-breaking heatwave event in summer 2017 over the Yangtze River Delta. *Bulletin of the American Meteorological Society*, *100*(1), S97–S103. https://doi.org/10.1175/BAMS-D-18-0134.1

Zhou, D., Liangxia, Z., Dan, L., Dian, H., & Chao, Z. (2016). Climate–vegetation control on the diurnal and seasonal variations of surface urban heat islands in China. *Environmental Research Letters*, *11*(7), 074009. https://doi.org/10.1088/1748-9326/11/7/074009

Zhou, D., Zhao, S., Zhang, L., Sun, G., & Liu, Y. (2015). The footprint of urban heat island effect in China. *Scientific Reports*, *5*, 11160. https://doi.org/10.1038/srep11160